Visualizing Interfacial Structure at Non-Common-Atom Heterojunctions with Cross-Sectional Scanning Tunneling Microscopy

J. Steinshnider and M. Weimer*
Department of Physics, Texas A&M University, College Station, Texas 77843

R. Kaspi
Air Force Research Laboratory, AFRL/DELS, Kirtland Air Force Base, Albuquerque, New Mexico 87117

G. W. Turner
Lincoln Laboratory, Massachusetts Institute of Technology, Lexington, Massachusetts 02173

(Received 23 December 1999)

We describe how cross-sectional scanning tunneling microscopy (STM) may be used to image the interfacial bonding across the nearly lattice-matched, non-common-atom GaSb/InAs heterojunction with atomic-scale precision. The method, which takes advantage of the length difference between interfacial and bulk bonds, appears equally applicable to AlSb/InAs and suggests how one might recover the complete structure of either heterojunction from atomic-resolution STM data.

PACS numbers: 61.16.Ch, 68.35.Ct, 68.65.+g

The 6.1 Å III-V semiconductor family is of considerable scientific and technical interest because it embraces three, nearly lattice-matched binary compounds—GaSb, InAs, and AlSb—that, together with their alloys, can all be grown epitaxially [1,2]. Numerous opportunities for capitalizing on the unique electronic properties of these materials [3,4], especially the type-II band alignment between GaSb and InAs, have been recognized. Suitable control over the properties of GaSb/InAs or AlSb/InAs superlattices and quantum wells grown by molecular beam epitaxy (MBE) is nevertheless challenging for a number of reasons. Difficulties emerge because anions and cations both change across an interface between materials that have no atoms in common. The structural perfection of such non-common-atom interfaces is therefore susceptible to compromise through isovalent intermixing of either species.

Non-common-atom heterojunctions differ from their common-atom counterparts in another, more fundamental, regard as well. A compositionally abrupt GaSb/InAs interface, for example, introduces new bonding partnerships—either InSb-like or GaAs-like [5]—otherwise absent from the bulk. The nature of this interfacial bonding exerts an understandably powerful influence on the structural, vibrational, and electronic properties of GaSb/InAs [6–10], and AlSb/InAs [11–14], superlattices and quantum wells.

Cross-sectional scanning tunneling microscopy (STM) has previously been used to characterize compositional fluctuations [15,16], isovalent intermixing [17–20], and interfacial roughness [21–24] in a variety of III-V semiconductor heterostructures. Here, we show how STM may also be employed to identify the *interfacial bonding* at GaSb/InAs and AlSb/InAs heterojunctions.

It is a straightforward consequence of the disparity in bulk lattice constants between InSb (6.48 Å), GaAs (5.65 Å), and GaSb (6.10 Å), for instance, that atomically thin InSb- or GaAs-like layers coherently strained to GaSb are under in-plane compression or tension, respectively. The tetragonal distortion arising in these layers from the large mismatch in natural bond lengths with respect to the surrounding materials causes an increase or decrease of the average lattice constant that is apparent with high-resolution x-ray diffraction (HRXRD) [6,7]. We argue that local relaxation of this strain following cleavage restores the bond angles between individual pairs of top-layer and subsurface atoms to their natural value, thereby enabling direct, atomic-scale visualization of the interfacial arrangement at these heterojunctions.

The principal structure considered in this study—a ten-period GaSb/InAs multiple quantum well (MQW)—was fabricated in a solid-source MBE system equipped with arsenic and antimony crackers. The sample consisted of a 0.1 μm Be-doped GaSb buffer layer, grown on top of an (001)-oriented p-type GaSb substrate, followed by ten 40 monolayer (ML) GaSb/14 ML InAs repeats and a 0.1 μm GaSb cap. The MQW layers were deposited just above the temperature at which the static, Sb-rich GaSb surface displays a 1×5 to 1×3 reconstruction transition, using growth rates of 0.5 ML/s for each material. The resulting HRXRD spectrum exhibited sharp MQW peaks whose splitting indicated a [001] periodicity in good agreement with that expected for a nominal 40/14 quantum well.

Each GaSb-on-InAs heterojunction in the structure was subjected to a 12 sec Sb_2 soak (with the Ga shutter closed) to promote antimony-for-arsenic exchange and the formation of InSb-like interface bonds. A 2 sec total growth interrupt was employed at each InAs-on-GaSb interface, after which the As and In shutters were simultaneously opened, and the low growth temperature relied upon to quench arsenic-for-antimony exchange so that InSb-like interface bonds were again favored. Both sets of interfaces

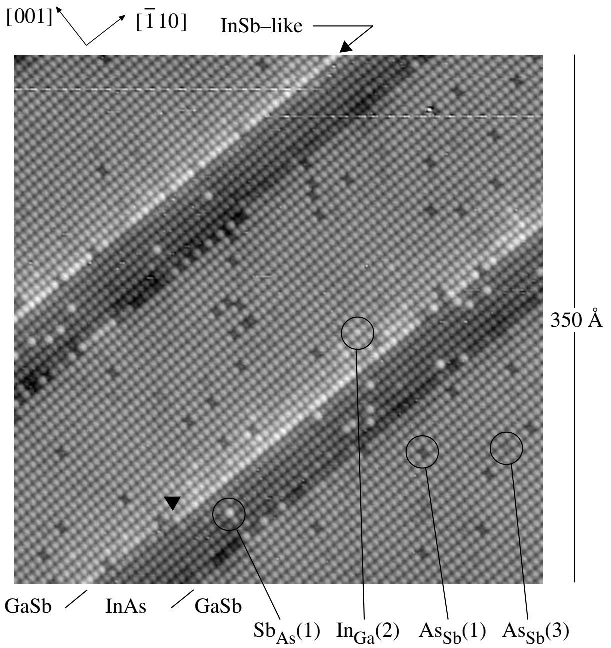

FIG. 1. Anion sublattice image of GaSb/InAs quantum wells in (110) cross section. InSb-like bonds account for the bright antimony layer along each GaSb-on-InAs interface. Growth direction is [001].

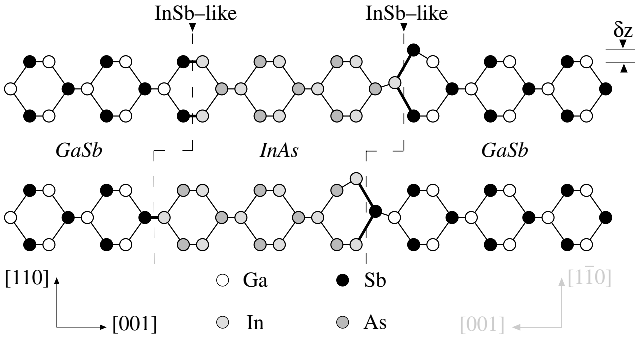

FIG. 2. Schematic GaSb/InAs quantum well illustrating the connection between growth sequence, cleavage direction, and InSb-like bond orientation. Normal and shaded axes denote (110) and $(1\bar{1}0)$ cleavage surfaces, respectively, dotted lines the monolayer fluctuations along each interface.

were exposed in cross section by cleavage along either a (110) or $(1\bar{1}0)$ plane in a separate UHV STM chamber and subsequently imaged with positive as well as negative sample bias.

Figure 1 shows a high-resolution, (110) view of the quantum wells and their interfaces using a sample bias chosen to image the filled-state density associated with As and Sb. The overwhelming majority of these top-layer atoms lie in a common plane by virtue of the near lattice match between InAs and GaSb, and the pronounced contrast between materials is an electronic effect [25]. The bulklike isovalent impurities introduced during epitaxy—arsenic-for-antimony ($\mathrm{As}_{\mathrm{Sb}}$) substitutions from cross incorporation [19], antimony-for-arsenic ($\mathrm{Sb}_{\mathrm{As}}$) substitutions due to anion segregation [26], and indium-for-gallium ($\mathrm{In}_{\mathrm{Ga}}$) substitutions due to cation segregation [17,18]—present a different situation, however. These impurities are conveniently specified by noting the crystal plane in which a given substitution occurs, so that $\mathrm{Sb}_{\mathrm{As}}(1)$, for example, refers to antimony-for-arsenic replacement in the cleavage-exposed top layer, $\mathrm{In}_{\mathrm{Ga}}(2)$ indium-for-gallium replacement in the (110) plane immediately beneath the cleavage surface [18], and so on.

We now point to an obvious correspondence between the STM signatures associated with these bulklike isovalent impurities and the signature one might expect of a lattice-mismatched interface. We note that at either an $\mathrm{Sb}_{\mathrm{As}}(1)$ or $\mathrm{In}_{\mathrm{Ga}}(2)$ site, each of which appears especially bright in Fig. 1, a lattice-matched InAs- or GaSb-like back bond is replaced with a *longer* InSb-like one that pushes a top-layer Sb atom above the surface plane defined by the surrounding anions [27]. We therefore similarly associate the bright row of Sb atoms along each of the GaSb-on-InAs heterojunctions in Fig. 1 with InSb-like interface bonds.

This geometric identification is supported with topographic sections indicating a change in tip height across the GaSb-on-InAs interface (δz in Fig. 2) of 0.25 ± 0.02 Å (within a -2.0 to -2.5 V tunneling window), in close agreement with a [110]-projected change of 0.27 Å based on the difference between second-nearest-neighbor distances [28] in unstrained InSb and GaSb. (This comparison overlooks the Jahn-Teller surface relaxation following cleavage—omitted from Fig. 2 for simplicity—but it is well established these displacements scale linearly with the bulk lattice constant [29]; it likewise overlooks any perturbation in the rehybridization of the anion dangling bonds due to asymmetric bond-length-induced distortions of this rigid-bond rotation.)

The data in Fig. 1 raise two additional questions that bear on this identification, however. First, why are the otherwise-bright Sb sites along the lower GaSb-on-InAs heterojunction missing at (among other places) the interfacial kink (marked with a carat) in this image? Second, why are all of the supposedly InSb-like bonds along both InAs-on-GaSb heterojunctions missing as well?

A reasonable answer to the first question quickly emerges from inspection of Fig. 2. The InSb-like back bonds exposed by (110) cleavage of a GaSb-on-InAs heterojunction alternate between *anion*-on-top (top) and *cation*-on-top (bottom) pairings with each monolayer shift in the position of this interface. Thus, from the viewpoint

TABLE I. Connection between growth sequence, bond type, and cleavage surface with out-of-plane interface bonds. Presumed growth direction is [001].

	GaSb-on-InAs (inverted)	InAs-on-GaSb (normal)
InSb-like	(110)	$(1\bar{1}0)$
GaAs-like	$(1\bar{1}0)$	(110)

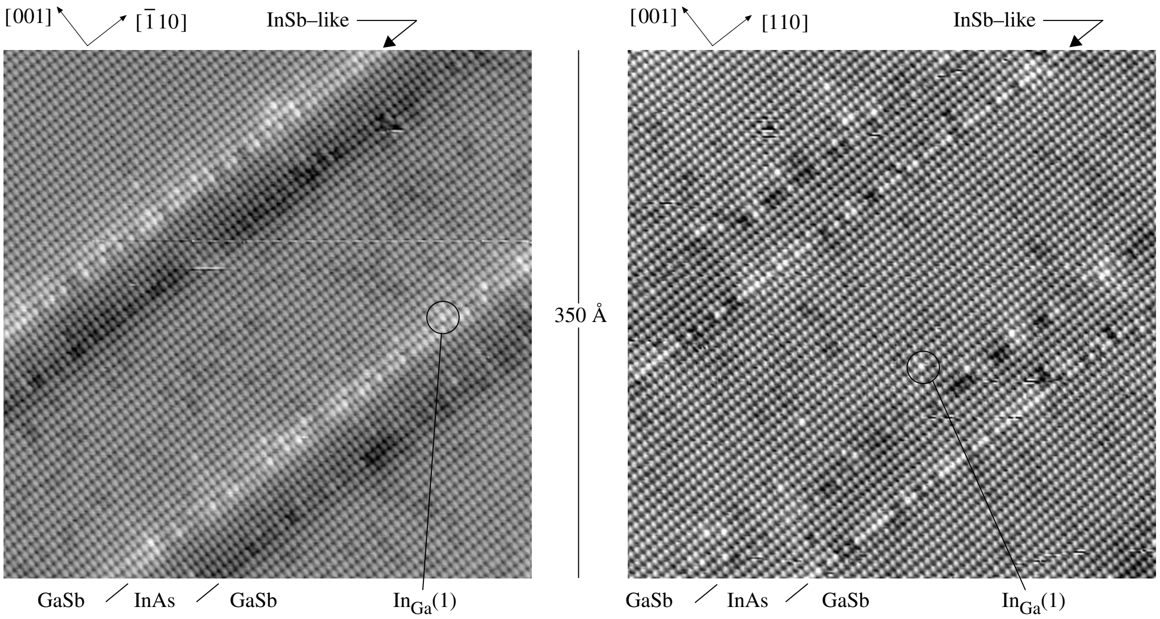

FIG. 3. Cation sublattice images of GaSb/InAs quantum wells in orthogonal (110) and (1$\bar{1}$0) cross sections. The InSb-like signature along each well shifts between GaSb-on-InAs and InAs-on-GaSb heterojunctions mirroring the dependence of interface-bond orientation on cleavage direction (Fig. 2).

of the Sb sublattice alone, monolayer islanding in the growth plane appears as a switch from InSb- (bright) to GaSb-like (normal) character, and vice versa, along the visible "interface."

The second question is more subtle. As illustrated in Fig. 2, and summarized in Table I, the tetrahedral coordination of the zinc blende lattice imposes fixed connections between the growth sequence, interface bond type, and crystallographic plane in which these bonds form. Thus, whether the InSb-like bonds at an InAs-on-GaSb heterojunction, for example, possess in- or out-of-plane orientation depends on whether we choose a (110) or orthogonal (1$\bar{1}$0) cleavage face (Table I). For a MQW with nominally even numbers of GaSb and InAs monolayers, *out-of-plane* InSb-like bonds at the (inverted) GaSb-on-InAs heterojunction will coincide with *in-plane* InSb-like bonds at the (normal) InAs-on-GaSb heterojunction (Fig. 2). The virtual absence of InSb-like character along the InAs-on-GaSb interfaces in Fig. 1 (apart from Sb segregation) leaves only two possibilities: either our initial presumption is incorrect, and the InAs-on-GaSb interface is instead GaAs-like (with, for example, cations on top), or the normal heterojunction is InSb-like, as intended, but (essentially) none of the extension associated with these bonds is directed toward the STM tip. The second circumstance is easily tested.

Figure 3 presents contrasting (110) and (1$\bar{1}$0) views of the normal and inverted heterojunctions using a sample bias chosen to image the empty-state density originating with In and Ga. Though the two images exhibit somewhat different layer contrasts (a property particularly sensitive to the condition of one's tip), the overwhelmingly InSb-like character of the InAs-on-GaSb interface is nonetheless strikingly confirmed in (1$\bar{1}$0) cross section, as is the crucial role played by the out-of-plane orientation of these bonds in their subsequent detection with STM. That this indisputably InSb-like character remains undisclosed in (110) cross section despite imaging both anion (Fig. 1, negative sample bias) *and* cation (Fig. 3, left, positive sample bias) sublattices is consistent with bond-length-preserving strain relaxation, but would seemingly preclude any electronic state associated with an InSb-like interface as a likely explanation for these data.

Complementary evidence for the lattice-mismatch-driven character of the interface-bond signatures in Figs. 1 and 3 comes from comparison of the non-common-atom InAs-on-GaSb heterojunction with its common-atom counterpart, AlSb-on-GaSb, where these bonds are the same length as those in the materials on either side. As suggested with the contrasting cation sublattice perspectives reproduced in Fig. 4, STM images of the *common-atom* interface are remarkably featureless.

These results, while clearly of fundamental interest, also convey important insights concerning the level of control presently exercised over interfacial structure in the 6.1 Å material system. Comparison of the cation sublattice images in Fig. 3, for example, indicates the InAs-on-GaSb interface is compositionally abrupt, whereas the GaSb-on-InAs interface is graded due to In segregation (also visible in Fig. 1); this asymmetry is the (not surprising) cation counterpart to the anion-sublattice asymmetry [30] introduced by Sb segregation. More intriguing is the surely related observation that the cleavage-exposed, InSb-like character along the normal interface (~75% in

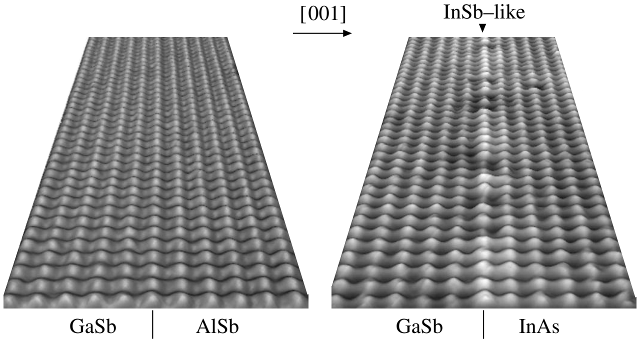

FIG. 4. Three-dimensional rendering of the cation sublattices along the common-atom AlSb-on-GaSb (left) and non-common-atom InAs-on-GaSb (right) interfaces.

large-area cation surveys) is considerably greater than that along the inverted one (~50% in large-area anion surveys). Of note, too, are the dark inclusions scattered at various points along the InAs-on-GaSb heterojunctions in Figs. 1 and 3 (left). These features (whose frequency exceeds the background from As cross incorporation) are consistent (Table I) with *shorter* GaAs-like bonds attributable to incomplete quenching of arsenic-for-antimony exchange. Finally, there are obvious parallels linking many of the phenomena described here with those that occur at AlSb/InAs heterojunctions whose interfaces may be either InSb- or AlAs-like, and these circumstances have likewise been observed with cross-sectional STM [31].

Of potentially greater significance, however, is the following point suggested by the structural logic on which our identification of InSb- and GaAs(AlAs)-like bonds rests. Interface meandering (with fixed composition) results in a transfer of the lattice-mismatched back bonds detected with STM from one sublattice to the other (Fig. 2); a change in interface type, on the other hand, results in a reorientation of these bonds (Table I) that causes their disappearance altogether. Thus, one could conceivably take advantage of this ability to pinpoint the bonds that define a GaSb/InAs or AlSb/InAs interface to recover the complete structure of either heterojunction, using the combined information from anion and cation sublattices [32] to answer both "where is the interface?" and "what is its composition?"

In conclusion, we have shown how cross-sectional STM can be used to characterize the lattice-mismatched bonding across the non-common-atom GaSb/InAs and AlSb/InAs interfaces with atomic-scale precision, and described how such measurements advance our understanding of the connection between interfacial structure, interfacial chemistry, and the growth conditions used to form these complex heterojunctions.

The authors are indebted to J. Harper, D. H. Chow, and T. C. Hasenberg for valuable discussions. STM characterization at Texas A&M University is supported by the National Science Foundation (DMR-9633011) and Air Force Research Laboratory (AFRL). MBE growth at AFRL is made possible by Air Force Office of Scientific Research support of the shared facility at the University of New Mexico. MBE growth at Lincoln Laboratory is supported by AFRL.

---

*Email address: weimer@tamu.edu

[1] C.-H. Chang *et al.,* Appl. Phys. Lett. **31**, 759 (1977).
[2] C.-A. Chang *et al.,* Appl. Phys. Lett. **40**, 983 (1982).
[3] L. L. Chang and L. Esaki, Surf. Sci. **98**, 70 (1980).
[4] L. Esaki, L. L. Chang, and E. E. Mendez, Jpn. J. Appl. Phys. **20**, L529 (1981).
[5] A. Fasolino, E. Molinari, and J. C. Maan, Phys. Rev. B **33**, 8889 (1986).
[6] B. R. Bennett *et al.,* Appl. Phys. Lett. **63**, 949 (1993).
[7] N. Herres *et al.,* Phys. Rev. B **53**, 15 688 (1996).
[8] S. G. Lyapin *et al.,* Phys. Rev. Lett. **74**, 3285 (1995).
[9] L. A. Hemstreet, C. Y. Fong, and J. S. Nelson, J. Vac. Sci. Technol. B **11**, 1693 (1993).
[10] B. R. Bennett *et al.,* Solid State Electron. **37**, 733 (1994).
[11] I. Sela *et al.,* Appl. Phys. Lett. **60**, 3283 (1992).
[12] R. G. Dandrea and C. B. Duke, Appl. Phys. Lett. **63**, 1795 (1993).
[13] B. Brar *et al.,* Appl. Phys. Lett. **64**, 3392 (1994).
[14] B. R. Bennett, B. V. Shanabrook, and E. R. Glaser, Appl. Phys. Lett. **65**, 598 (1994).
[15] H. W. M. Salemink and O. Albrektsen, Phys. Rev. B **47**, 16 044 (1993).
[16] K. J. Chao *et al.,* Phys. Rev. Lett. **79**, 4822 (1997).
[17] J. F. Zheng *et al.,* Phys. Rev. Lett. **72**, 2414 (1994).
[18] M. Pfister *et al.,* Appl. Phys. Lett. **67**, 1459 (1995).
[19] J. Harper *et al.,* J. Vac. Sci. Technol. B **16**, 1389 (1998).
[20] H. Chen *et al.,* Appl. Phys. Lett. **75**, 79 (1999).
[21] R. M. Feenstra *et al.,* Phys. Rev. Lett. **72**, 2749 (1994).
[22] S. L. Skala *et al.,* J. Vac. Sci. Technol. B **13**, 660 (1995).
[23] A. Y. Lew *et al.,* Phys. Rev. B **57**, 6534 (1998).
[24] J. Harper *et al.,* Appl. Phys. Lett. **73**, 2805 (1998).
[25] R. M. Feenstra *et al.,* J. Vac. Sci. Technol. B **12**, 2592 (1994).
[26] J. Steinshnider *et al.* (to be published).
[27] There is, of course, an additional electronic component to the $\mathrm{Sb}_{\mathrm{As}}(1)$ signature associated with replacement of an As dangling bond by an Sb one.
[28] See, for example, M. C. Schabel and J. L. Martins, Phys. Rev. B **43**, 11 873 (1991).
[29] C. B. Duke, J. Vac. Sci. Technol. A **10**, 2032 (1992).
[30] M. W. Wang *et al.,* J. Vac. Sci. Technol. B **13**, 1689 (1995).
[31] J. Steinshnider, M. Weimer, and G. W. Turner (unpublished).
[32] R. M. Feenstra *et al.,* Phys. Rev. Lett. **58**, 1192 (1987).